# ASSESSMENT OF STEC ESTIMATION QUALITY USING GNSS PPP FIXED

J. F. Galera Monico [1*,] P. S. de Oliveira Jr [2], V. A. Stuani Pereira [3], S. B. L. Machado [1]

[1] Universidade Estadual Paulista - Unesp, Presidente Prudente, SP, Brazil - (galera.monico, brian.leite)@unesp.br
[2] Universidade Federal do Paraná - UFPR, Curitiba, PR, Brasil - paulo.junior@ufpr.br
[3] Universidade Tecnológica Federal do Paraná - UTFPR, Santa Helena, PR, Brazil - vpereira@utfpr.edu.br

**KEY WORDS:** GNSS, PPP, STEC, Quality analysis, Space Weather.

**ABSTRACT:**

GNSS (Global Navigation Satellite System) data can be used for geodetic remote sensing, particularly for monitoring the ionosphere in the context of Space Weather. One of the important parameters derived from GNSS measurements for ionospheric analysis is the Slant Total Electron Content (STEC). By utilizing GNSS data from multiple frequencies or even a single frequency, the STEC can be computed using an appropriated linear combination, like geometry free. However, when computing an ionospheric gradient between two IPP (Ionospheric Pierce Point) from the same satellite, the precision of the STEC estimate can become a limiting factor. In some cases, the uncertainty in the estimate may be greater than the actual gradient value itself. This poses challenges, especially for augmentation systems like GBAS (Ground Based Augmentation System), where accurate ionospheric gradients are crucial. An alternative approach to improve these limitations is to estimate the STEC using a different approach, like Precise Point Positioning (PPP). For such case, the coordinates of the GNSS stations are constrained to known values (PPP-Fixed), while other parameters such as clock biases, tropospheric delays, and ionospheric delays (including STEC) can be estimated. The results of an experiment carried out to assess the quality of STEC for such application are presented and have shown good results. Ionospheric gradients are agreed in the mm level.

## 1. INTRODUCTION

### 1.1 The problem to be solved

GNSS (Global Navigation Satellite System) data can be used for geodetic remote sensing, particularly for monitoring the ionosphere in the context of Space Weather. One of the important parameters derived from GNSS measurements for ionospheric analysis is the Slant Total Electron Content (STEC). By utilizing GNSS data from multiple frequencies or even a single frequency, the STEC can be computed.

The estimation of STEC is typically performed by combining the pseudorange and phase measurements of the carrier wave using a geometry free linear combination. When employing dual frequency, relevant studies such as (Yasyukevich et al. 2015) and (Tuna et al. 2014) provide detailed insights into the methodology. For single frequency TEC computation, Hein et al. (2016) is a good start point, together with Christovam et al. (2023) that used the approach for plasma bubbles imaging. With this methodology, the expected accuracy of STEC estimation is usually around 2 TECU (TEC Units) or higher, which is equivalent to approximately 32 cm at the L1 frequency (1575.42 MHz). This level of uncertainty can be observed in IONEX ( IONosphere map EXchange) files available by IGS (International GNSS Services), used for exchanging ionosphere maps within the IGS community (Johnston et al. 2017).

However, when computing an ionospheric gradient between two IPP (Ionospheric Pierce Point) from the same satellite (time-step method), the precision of the STEC estimate can become a limiting factor. In some cases, as the uncertainty in the estimate may be greater than the actual gradient value itself. This poses challenges, especially for augmentation systems like GBAS (Ground Based Augmentation System), where accurate ionospheric gradients are crucial for developing ionospheric threat models (Balvedi et al. 2016).

To mitigate this problem, it is desirable to have STEC estimates with higher levels of accuracy, typically in the order of a few centimetres. By improving the precision of the estimate, the statistical significance of ionospheric gradients can be preserved, enabling more reliable applications such as GBAS threat model.

### 1.2 Proposed solution

An alternative approach to improve the limitations mentioned earlier is to estimate the STEC using Precise Point Positioning (PPP) (Li et al. 2022; Oliveira Jr et al. 2023). For such case, the coordinates of the GNSS stations can be constrained to known values or even fixed (PPP-Fixed). Other GNSS processing parameters can be neglected or estimated depending on the PPP variant used. Among these noteworthy parameters, it is essential to highlight tropospheric delays which can be estimated along with horizontal tropospheric gradients (Morel et al. 2021), slant ionospheric delays (STEC) (Oliveira Jr 2017), clock biases or even inter-system biases when processing multiple GNSS (multi-GNSS) constellations data (Setti Jr et al. 2020; Li et al. 2022). Precise ephemerides and clocks have to be obtained from external founts, like IGS.

In the case of GNSS PPP-Fixed, the ambiguities can be resolved as either integer (PPP-AR) or real (PPP-AF), depending on the level of precision required. By employing PPP, it is possible to obtain more accurate estimates of STEC, which can help address the issue of limited statistical significance in ionospheric gradients.

Additionally, it is important to consider that the estimated STEC values obtained through PPP will still contain biases originating from the receiver and satellite. For many applications these biases from the ionospheric observables need to be estimated and corrected to obtain accurate ionospheric delays. These observables, which include the corrected STEC values, are essential for various applications in Space Weather monitoring and augmentation systems. In order to assess fast ionospheric variabilities, such as for ionospheric gradients purposes,

hardware biases could be estimated previously and mitigated from real-time ionospheric observables. For this specific application, one also could neglect receiver instrumental biases affecting ionospheric observables, since these biases vary slowly and will not affect quick ionospheric delay variations observed throughout ionospheric gradients.

### 1.3 Objective

The main objective of this work is to evaluate the quality of the STEC estimates obtained using ionospheric observables derived from GNSS PPP-fixed for application like in the GBAS gradient analysis.

### 2. FUNDAMENTALS ON STEC COMPUTATION

As already stated, the conventional estimation of STEC is performed by combining the pseudorange and phase measurements of the carrier wave using the geometry free observable. When using dual frequency, like L1 and L5 (L2) from GPS, or E1 and E5 from Galileo, it is quite easy to compute such values, which have to be calibrated in order to take the biases into account (Yasyukevich et al. 2015).

Alternatively, once can compute the STEC from the PPP model (ionospheric observable). In this approach ionospheric delays are basically introduced as additional parameters to be estimated throughout the GNSS observables processing. Usually, the S-system theory is applied in order to allow the estimation of a greater number of parameters and solve to the rank defect (Psychas and Verhagen 2020). Once the ionospheric observables are available, the calibration of the bias can be performed, or one can also compute the ionospheric gradients without calibration, an important parameter for GBAS.

### 3. METHODOLOGY

To test the proposed methodology, an experiment was carried out in the Laboratory of Space Geodesy (LGE) located at Unesp in Presidente Prudente, SP, Brazil. Four GNSS receivers multifrequency and multi-constellation from the same manufacturer (Figure 1 (a) and (b)) were attached to the same antenna (Figure 1 (d) via a splitter (Figure 1 (c)). Data were collected during few days using the same configuration for all receivers.

Figure 2 shows the main information involved in the configuration. As once can see, whenever possible, (data + pilot) and (I+Q) were the chosen configurations. Data was converted from binary original format to RINEX 3.03.

Ionospheric observables, which can be converted to STEC values, were estimated for each satellite and receivers. We choose to apply the PPP-fixed strategy from RTKLib in a post processing mode (Takasu 2013). So, we used the forward and backward approach, using the estimated ambiguities in the forward process as input for the backward process. Of course, that it will not be the case for real time application, but it is quite important in this assessment process, as the precision will be at the same range as if it were PPP-AR. So far, RTKLib, does not allow PPP-AR.

Therefore, the station coordinates are fixed to their known values, reducing the number of parameters to be estimated within the GNSS data processing. Besides, this absolute constraint, applied to the coordinates of the station, allows a faster solution

convergence as well documented in related literature (Oliveira Jr 2017; Psychas and Verhagen 2020).

For the four collocated receivers we assessed the ionospheric observables estimates obtained by PPP processing using the Kalman filter settled as "combined (forward+backward) with no phase reset" strategy, as stated before. Since the four receivers are connected to the same GNSS antenna, existing differences between their slant ionospheric observables are considered to be produced mostly by receivers' hardware biases, including the splitter.



**Figure 1.** The experiment configuration at Unesp PP - Brazil.

| Type | Signal | Enable | Options |
|---|---|---|---|
| GPS | L1 - C/A | ☑ | |
| GPS | L1C | ☑ | |
| GPS | L2E | ☑ | L2C and L2E ▾ |
| GPS | L2C | ☑ | CM + CL ▾ |
| GPS | L5 | ☑ | I + Q ▾ |
| SBAS | L1 - C/A | ☑ | |
| SBAS | L5 | ☑ | |
| GLONASS | L1 - C/A | ☑ | |
| GLONASS | L1P | ☑ | |
| GLONASS | L2P | ☑ | L2 - C/A(M) and P ▾ |
| GLONASS | L2 - C/A | ☑ | |
| GLONASS | L3 | ☑ | Data + Pilot ▾ |
| Galileo | E1 | ☑ | Data + Pilot ▾ |
| Galileo | E5 - A | ☑ | Data + Pilot ▾ |
| Galileo | E5 - B | ☑ | Data + Pilot ▾ |
| Galileo | E5 - AltBOC | ☑ | Data + Pilot ▾ |
| Galileo | E6 | ☑ | Data + Pilot ▾ |
| BeiDou | B1 | ☑ | |
| BeiDou | B1C | ☑ | |
| BeiDou | B2 | ☑ | |
| BeiDou | B2A | ☑ | |
| BeiDou | B2B | ☑ | |
| BeiDou | B3 | ☑ | |

**Figure 2.** Main configurations of the Receivers.

The dispersion (standard deviations) of such differences also could precisely indicate the expected quality for resulting ionospheric observables. The gradients are computed as detailed in (Pereira et al. 2021) using the time steep procedure.

For the evaluation of ionospheric observables, only solutions of ionospheric observables with formal precisions better than 05 cm were used.

Subsequently, an experiment was conducted to assess the effectiveness of the proposed approach during ionospheric scintillation events. The experiment was conducted at two stations, MOR3 and STPZ, both situated in the city of Presidente Prudente, Brazil, the same location as described in the earlier validation study. In the presence of intensified ionospheric activity (during scintillation), the PPP method faced challenges in estimating slant ionospheric delays. To enable the PPP solution to estimate ionospheric delays even during scintillation events, certain adaptations were implemented:

1) **Solution adapted 1 (GPS+Galileo):** the Signal-to-Noise Ratio (SNR) mask was set at 38 dB, and the threshold for rejecting observations based on residuals was raised to 75 meters from the previous value of 30 meters.

2) **Solution adapted 2 (GPS+Galileo+GLONASS):** the unique modification was to increase the threshold for rejecting observations based on residuals to 75 meters, as opposed to the previous threshold of 30 meters.

## 4. PRELIMINARY RESULTS

GNSS data from day 152 of 2023 were used to provide the preliminary assessment of the results. The precision of the biased STEC for data without scintillation was of the order of few centimetres. In the sequence, we computed the slant gradients together with the respective precision for a group of satellites. For the gradient's computation, we considered GPS from blocks IIR-M, IIF and GPS-III.
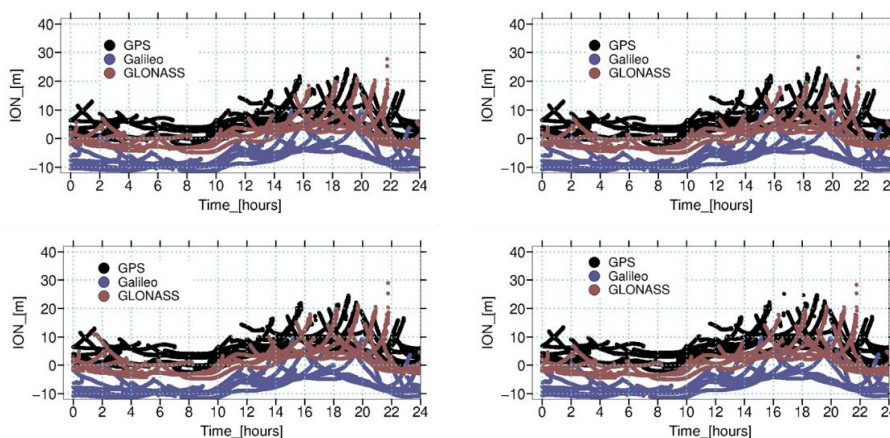


**Figure 3.** Slant ionospheric delays estimated for GNSS receivers from stations PPT2 (top-left), PPT3 (top-right), PPT4 (bottom-left) and PPTE (bottom-right), day of year 152/2023.

The differences between PPTE and the other stations presented an interesting dispersion with quality close to 01 ~ 02 cm, especially for GPS and Galileo constellations. The daily mean and the standard deviations of these epoch-wise differences were about the same quality for all the assessed period, as one can see in Table 1 respectively. Most differences found in this test presented biases with an amplitude ranging from centimetres to a few decimetres. This indicates that receiver hardware bias differences could be present, even though they are of the same brand and with similar configuration. Therefore, receiver hardware biases were estimated by applying to the ionospheric observables, the algorithm implemented in (Oliveira Jr et al. 2020).

Figure 5 shows the results of the individual estimation using ionospheric observables obtained for each receiver separately. Receiver hardware biases for Galileo and GPS constellations presented more stability in terms of variations. Besides, hardware biases for the 3 constellations showed similar behaviors expected because: 1) all the receivers are the same brand & model and 2) the 4 receivers are connected to the same antenna as well.

Figure 3 presents the slant ionospheric observables obtained through PPP processing for GPS, GLONASS and Galileo satellites. It is possible to see clearly the expected daily pattern for the estimated ionospheric parameters. This is an important aspect to consider for the ionospheric observables' validation, since ionospheric observables obtained from this strategy (PPP processing) could not reflect typical ionospheric behaviour if the estimability of such a parameter was compromised. As expected, another important remark is the degree of similarity among ionospheric delays estimated using GNSS data from the four receivers (PPTE, PPT2, PPT3 and PPT4) involved in the experiment. As shown in Figure 3, the estimated ionospheric observables presented very similar results for the three GNSS constellations: GPS, GLONASS and Galileo. Besides, an inter constellation bias is also visible, and the presence of negative values is usually caused by hardware biases, which are generally absorbed by ionospheric observables.

Figure 4 brings the resulting differences between slant ionospheric observables estimated at the PPTE receiver with respect to the three other receivers in our study (PPT2, PPT3 and PPT4). As already stated, these differences are computed only for ionospheric observables with formal precisions better than 5 cm.

In the sequence, we computed the slant ionospheric gradients together with the respective precision for a group of satellites. We consider GPS satellites from blocks IIR-M, IIF and GPS-III. Results for satellites PRN 17 (IIR-M), PRN 32 (IIF) and PRN 11 (GPS-III) are shown in Figure 6. One cannot observe any significant difference from these blocks of satellites. And, although the magnitude of the corresponding ionospheric gradients can be considered small, the precision level makes them considerably robust.

In Figure 6 it is possible to remark that gradients (in blue) for the four receivers are very similar. Their differences do not exceed 1 mm. This indicates that existing hardware biases affecting slant ionospheric observables do not influence ionospheric gradients results. This is expected since

ionospheric gradients only show the variability of slant ionospheric delays. Thus, the relevant aspect to be considered when computing ionospheric gradients is the precision of the provided slant ionospheric observables and we have confirmed this with results shown in Figure 6.
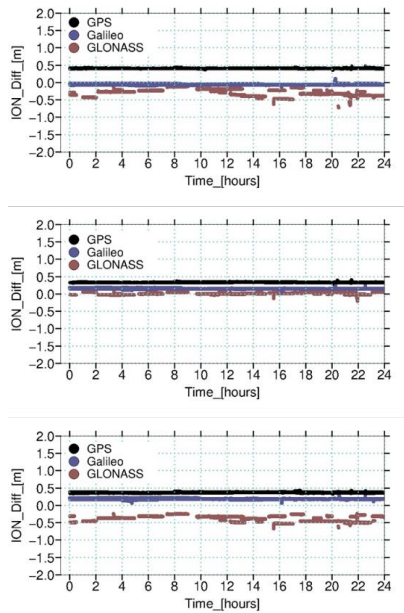


**Figure 4.** Slant ionospheric delay differences between GNSS receivers from stations PPTE and PPT2 (top), PPT3(middle) and PPT4 (bottom), DoY 152/2023.

Finally, Figure 7 presents the formal precision of ionospheric gradients obtained for GNSS constellations: GPS (top), GLONASS (middle) and Galileo (bottom). Results are presented for all visible satellites used to compute the gradients at station location during day 152/2023. These outcomes were obtained by covariance propagation using the gradients equation model (time step), applied to the estimated precision of the input slant ionospheric observables. Yet in Figure 7 one can observe that the formal precision of the ionospheric gradients varies from 2 mm/km to about 16 mm/km. The ionospheric gradients for ionospheric observables of the Galileo constellation were slightly less precise than those from GLONASS or GPS constellations.

| Doy | PPTE-PPT2 | | PPTE-PPT3 | | PPTE-PPT4 | |
|-----|-----------|--------|-----------|--------|-----------|--------|
|     | Mean[m]   | STD[m] | Mean[m]   | STD[m] | Mean[m]   | STD[m] |
| 152 | 0.41      | 0.01   | 0.34      | 0.01   | 0.37      | 0.01   |
| 156 | 0.41      | 0.01   | 0.34      | 0.01   | 0.38      | 0.01   |
| 160 | 0.41      | 0.01   | 0.33      | 0.01   | 0.38      | 0.01   |
| 166 | 0.39      | 0.02   | 0.31      | 0.02   | 0.31      | 0.02   |
| 172 | 0.41      | 0.01   | 0.33      | 0.01   | 0.39      | 0.01   |

**Table 1.** Statistics of the differences between slant ionospheric observables for GPS satellites.

| Doy | PPTE-PPT2 | | PPTE-PPT3 | | PPTE-PPT4 | |
|-----|-----------|--------|-----------|--------|-----------|--------|
|     | Mean[m]   | STD[m] | Mean[m]   | STD[m] | Mean[m]   | STD[m] |
| 152 | -0.06     | 0.02   | 0.15      | 0.01   | 0.18      | 0.02   |
| 156 | -0.09     | 0.01   | 0.15      | 0.01   | 0.17      | 0.02   |
| 160 | -0.08     | 0.02   | 0.14      | 0.02   | 0.17      | 0.02   |
| 166 | -0.06     | 0.02   | 0.12      | 0.01   | 0.18      | 0.02   |
| 172 | -0.07     | 0.01   | 0.14      | 0.01   | 0.18      | 0.02   |

**Table 2.** Statistics of the differences between slant ionospheric observables for Galileo satellites.

| Doy | PPTE-PPT2 | | PPTE-PPT3 | | PPTE-PPT4 | |
|-----|-----------|--------|-----------|--------|-----------|--------|
|     | Mean[m]   | STD[m] | Mean[m]   | STD[m] | Mean[m]   | STD[m] |
| 152 | -0.29     | 0.10   | 0.01      | 0.03   | -0.38     | 0.08   |
| 156 | -0.24     | 0.08   | 0.01      | 0.04   | -0.35     | 0.07   |
| 160 | -0.26     | 0.10   | 0.02      | 0.03   | -0.36     | 0.08   |
| 166 | -0.33     | 0.12   | 0.02      | 0.04   | -0.39     | 0.09   |
| 172 | -0.23     | 0.09   | 0.03      | 0.04   | -0.35     | 0.08   |

**Table 3.** Statistics of the differences between slant ionospheric observables for GLONASS satellites.
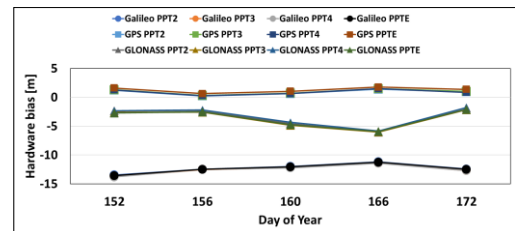


**Figure 5.** Estimated receiver hardware biases.

Subsequently, we present the results of experiment conducted to assess the proposed approach during ionospheric scintillation events, which occurred around midnight. As explained before, in the presence of intensified ionospheric activity, the PPP method faced challenges and two solutions were adapted in order to allow the method estimating slant ionospheric delays.

Figure 8 brings the estimated ionospheric delays at MOR3 station. Even with the adaptations, the estimated ionospheric delays for both solutions were very unstable around midnight, critical scintillation period. Solution adapted 2 was not able to continuously estimate ionospheric delays at this period. Results for station STPZ (not shown) were very similar.

Figure 9 presents the ionospheric gradients computed for both stations MOR3 and STPZ for GPS satellite PRN11 (GPS III), using the ionospheric observables of solution adapted 2. In this gradient computation, the adoption ionospheric observables in function of its formal precision, to compute gradients, considered a threshold of 10cm instead of 05cm. Otherwise, one could not have enough ionospheric observables to compute gradients. Results using solution adapted 1 are not shown, but they were very close as well. It is possible to remark that gradients amplitude could reach up to ~07cm/km keeping a formal precision of about 01cm. In Figure 10, the formal precisions for ionospheric gradients obtained throughout covariances propagation for all day long, for GPS constellation are showed. Solution adapted 2 has better performances in terms of precision. Both solutions were unable to produce ionospheric observables with formal standard deviations better than ~10mm/km, thus there are no gradients estimated during the most part of the critical scintillation period.

## 5. CONCLUSIONS AND PROSPECTS

In this study, the assessment of the ionospheric products obtained throughout PPP processing was accomplished. An experiment using four receivers connected to the same GNSS antenna was designed in order to evaluate the comparison of the ionospheric estimates generated using this strategy.
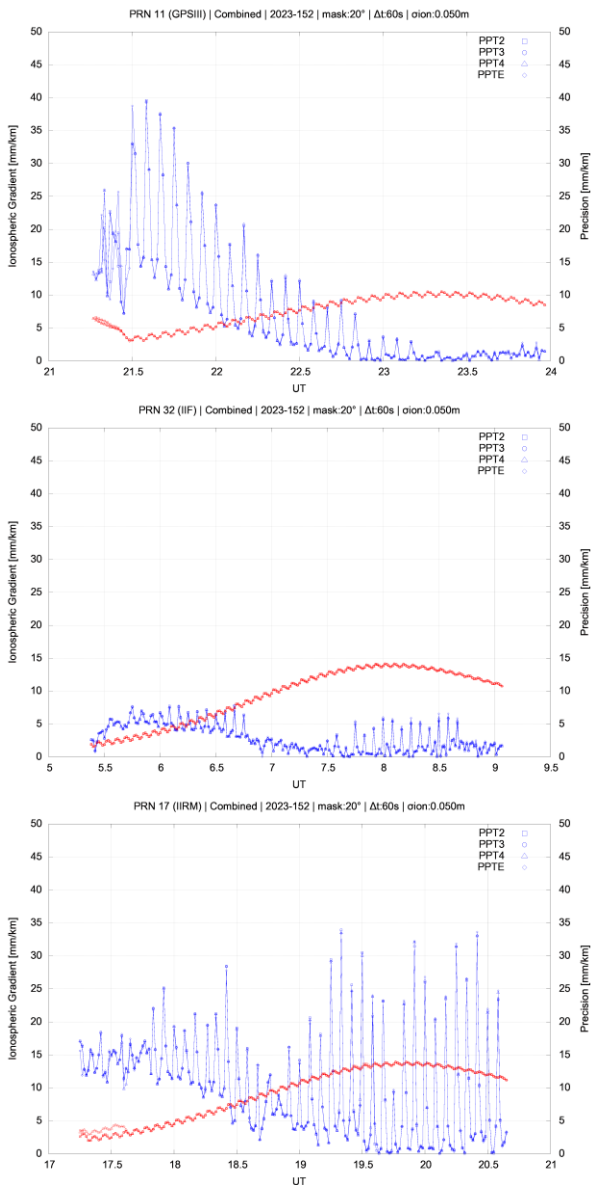
**Figure 6.** Ionospheric gradients (blue) and precisions (red) for GPS satellites PRN 17 (bottom) PRN 32 (middle) and PRN 11 (top).

The physical behaviour of the ionospheric expected characteristics as well as the quality of the derived ionospheric gradients was also evaluated. The assessment of the ionospheric gradients produced very similar ionospheric gradients (mm level) for all the four receivers involved in the test. This result allowed us to confirm that, when computing ionospheric gradients, one important aspect is to estimate the precision of the provided slant ionospheric observables. Additionally, an investigation of the strategy under strong scintillation activity was carried out indicating that adaptations of the stochastic model must be considered when estimating ionospheric observable throughout PPP under such scintillation conditions. Further analysis will be carried out using an expanded data set, in order to obtain more reliable conclusions.
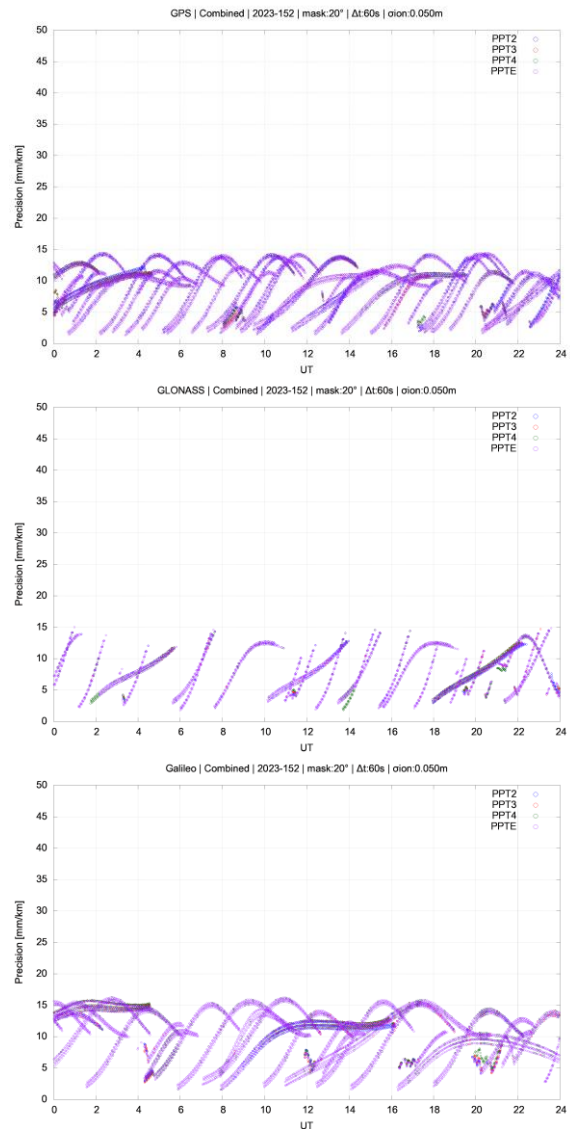


**Figure 7.** Formal precision of ionospheric gradients obtained for GNSS constellations GPS (top), GLONASS (middle) and Galileo (bottom), during day 152/2023.
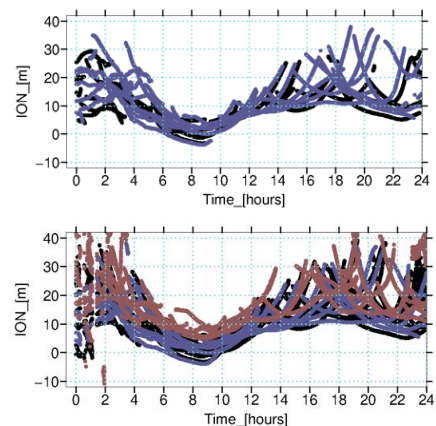


**Figure 8.** Slant ionospheric delays estimated for station MOR3: solution adapted 1 (top) and solution adapted 2 (bottom).
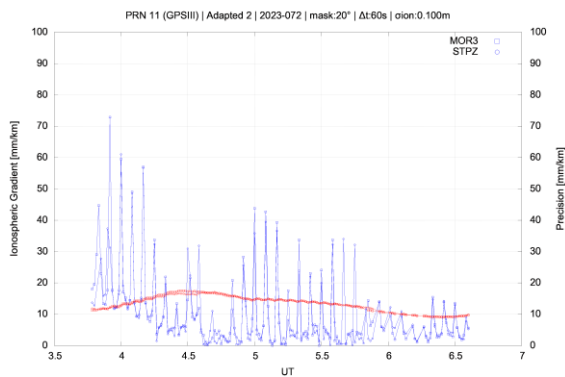
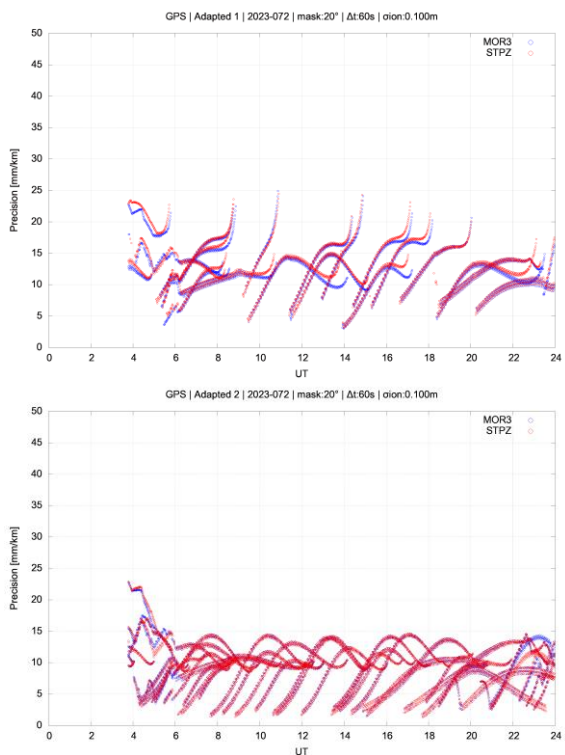**Figure 9.** Ionospheric gradients (blue) and precisions (red) for GPS satellite PRN 11.





**Figure 10.** Formal precision of ionospheric gradients obtained for GPS satellites: solution adapted 1 (top), and adapted 2 (bottom).

## REFERENCES

Balvedi, G.C., Harris, M., Peterson, W., Fregnani, J.A.G., Saotome, O. (2016) operational mitigation practice to enable the use of GBAS on areas influenced by harsh ionosphere phenomena. p 11

Christovam, A.L., Prol, F.S., Hernández-Pajares, M., Camargo, P.O. (2023) Plasma bubble imaging by single-frequency GNSS measurements. GPS Solut 27(3):124. https://doi.org/10.1007/s10291-023-01463-z

Hein, W.Z., Kashiwa, Y., Goto, Y., Kasahara, Y. (2016) Estimation method of ionospheric TEC distribution from single frequency GPS measurements using a slant effect model. In: 2016 URSI Asia-Pacific Radio Science Conference (URSI AP-RASC). pp 104–106

Johnston, G., Riddel, A., Hausler, G. (2017) The International GNSS Service. In: Teunissen, P., Montenbruck, O. (eds) Springer Handbook of Global Navigation Satellite Systems, 1st edn. Springer International Publishing, Cham, Switzerland

Li, X., Wang, B., Li, X., Huang, J., Lyu, H., Han, X. (2022) Principle and performance of multi-frequency and multi-GNSS PPP-RTK. Satell Navig 3(1):7. https://doi.org/10.1186/s43020-022-00068-0

Morel, L., Moudni, O., Durand, F., Nicolas, J., Follin, J-M., Durand, S., Pottiaux, E., Van Baelen, J., Sergio de Oliveira, P. (2021) On the relation between GPS tropospheric gradients and the local topography. ASR 68(4):1676–1689. https://doi.org/10.1016/j.asr.2021.04.008

Oliveira Jr, P.S., Monico, J.F.G., Morel, L. (2020) Mitigation of receiver biases in ionospheric observables from PPP with ambiguity resolution. ASR 65(8):1941–1950. https://doi.org/10.1016/j.asr.2020.01.037

Oliveira Jr, P.S. (2017) Definition and Implementation of a New Service for Precise GNSS Positioning. CNAM and Unesp. ⟨NNT : 2017CNAM1130⟩. ⟨tel-01695792⟩

Oliveira Jr, P.S., Morel, L., Galera Monico, J.F., Durand, S., Durand, F., Bezerra, L.D.S. (2023) An alternative to derive ionospheric and tropospheric SSR corrections for PPP-RTK using adaptive constraints. Survey Review :1–12. https://doi.org/10.1080/00396265.2023.2169063

Pereira, V.A.S., Monico, J.F.G., Camargo, P.D.O. (2021) Estimation and analysis of protection levels for precise approach at rio de janeiro international airport using real time σvig for each GPS and GLONASS satellite. Bol Ciênc Geod 27(spe):e2021010. https://doi.org/10.1590/s1982-21702021000s00010

Psychas, D., Verhagen, S. (2020) Real-Time PPP-RTK Performance Analysis Using Ionospheric Corrections from Multi-Scale Network Configurations. Sensors 20(11):3012. https://doi.org/10.3390/s20113012

Setti Jr, P. de T., Silva, C.M., Oliveira Jr, P.S., Alves, D.B.M., Monico, J.F.G. (2020) Multi-GNSS Positioning. RBC. 72:1200–1224. https://doi.org/10.14393/rbcv72nespecial50anos-56580

Takasu, T. (2013) RTKLIB ver. 2.4.2 Manual

Tuna, H., Arikan, O., Arikan, F., Gulyaeva, T.L., Sezen, U. (2014) Online user-friendly slant total electron content computation from IRI-Plas: IRI-Plas-STEC: TUNA ET AL. Space Weather 12(1):64–75. https://doi.org/10.1002/2013SW000998

Yasyukevich, YuV., Mylnikova, A.A., Polyakova, A.S. (2015) Estimating the total electron content absolute value from the GPS/GLONASS data. Results in Physics 5:32–33. https://doi.org/10.1016/j.rinp.2014.12.006